Environ. Sci. Technol. **1998**, *32,* 1333−1339

Analysis of Diffusion and Sorption of Organic Solutes in Soil-Bentonite Barrier Materials

ASHUTOSH KHANDELWAL, ALAN J. RABIDEAU,* AND PEILIANG SHEN†

Department of Civil, Structural, and Environmental Engineering, State University of New York at Buffalo, Amherst, New York 14260

A series of laboratory studies was conducted to assess the transport of chloride, trichloroethylene (TCE), and aniline in soil-bentonite (SB) slurry wall materials. Column transport experiments were conducted, with a primary emphasis on the measurement of spatial contaminant mass profiles within columns after 25−50 days of transport under diffusion-dominated conditions. The advective−dispersive−reactive (ADR) equation was found to provide good predictions of the results of the column experiments with calibrated diffusion parameters that were within the range observed by other researchers for earthen barrier materials. However, values of the porosity-corrected hindrance factor were higher than those observed in other studies of diffusive transport in SB, and sorption coefficients calibrated from the column experiments were significantly lower than values measured in batch isotherm tests conducted with unconsolidated SB. A number of factors could contribute to variability across experiments and investigators, including differences between batch and column conditions, differences in experimental apparatus and design used to study diffusive transport in SB, correlation between parameters in the calibration process, and the potential influence of nonequilibrium sorption in column experiments. For the design of conventional slurry walls, it is likely that conservative predictions of organic contaminant penetration can be obtained with the ADR equation using established correlations for effective diffusion coefficients and neglecting sorption to barrier materials.

Introduction

Soil-bentonite (SB) slurry walls frequently have been used to isolate hazardous contaminants from the surrounding environment and as integral components of engineered cleanup systems. Detailed discussions of the properties and applicability of SB barrier walls are available (*1, 2*). It is generally believed that if the hydraulic conductivity (K_h) of the SB wall is sufficiently low (less than 10^{-7} cm/s) and there are no structural cracks, the wall will be effective in curtailing the advective transport of contaminants. However, even if advective transport is insignificant, contaminants can migrate across the SB wall by molecular diffusion. Numerous studies have confirmed the importance of molecular diffusion in earthen barrier materials, in which effective diffusion coefficients typically are reduced by a factor of only 3−10 from their corresponding aqueous diffusion coefficients (*3−12*).

In analyzing diffusion in porous media, Millington (*13*) developed a correlation for estimating the medium hindrance as a function of porosity:

$$H_p = \frac{nD_o}{D_e} = n^{-e} \quad (1)$$

where H_p is a porosity-corrected hindrance factor (henceforth referred to as hindrance); n is the porosity; D_o is the free aqueous diffusion coefficient; D_e is the effective porous media diffusion coefficient, which reflects the reduction in cross-sectional area in addition to other factors; and e is a constant. For gas diffusion through fused-silica cylinders, Millington's proposed exponent was 0.33 (*13*) (adjusted for consistency with the notation of this work). Other exponents have been suggested for various porous media systems (*14, 15*). For earthen barrier materials, some investigators have observed lower effective diffusion coefficients than would be predicted from eq 1 with Millington's exponent (*9−11, 16*). In contrast, the diffusion coefficients obtained by Mott and Weber (*12*) for organic contaminants in SB were interpreted to be in accordance with Millington's exponent.

The physical characteristics of SB barriers are likely to be similar to those of other earthen barrier materials such as clay liners. Hence, the existing modeling approaches that utilize the advective−dispersive−reactive (ADR) equation for diffusion-dominated contaminant transport through clay liners can be extended to describe the migration of contaminants through SB barriers. The objectives of this research were to (a) assess the applicability of the one-dimensional ADR equation in predicting the migration of organic contaminants in SB barrier material, (b) assess the power function relationship for estimating diffusion coefficients for SB walls, (c) examine the applicability of independently measured sorption coefficients for predicting the migration of organic contaminants in SB, and (d) assess the applicability of low-gradient column experiments for measuring contaminant diffusion coefficients in SB. These objectives were addressed through a series of column transport and batch isotherm experiments using two organic contaminants and SB.

Experimental Methods

Materials. The backfill soil employed in this study was obtained from a local source and sieved to remove particles larger than 10 mesh (2 mm). The resulting soil was well graded and contained a high percentage of fines (45% passing 75 μm sieve) and was therefore deemed suitable for the use in slurry wall applications (*17*). The liquid and plastic limits of the backfill soil were 25 and 14%, respectively, and the organic content was measured at 1.3% (ASTM 2974-87). Industrial grade sodium bentonite was obtained from Fisher Scientific. The backfill soil and bentonite were mixed to achieve a bentonite content of 6 wt %, which is at the high end of the range recommended for slurry walls (*17, 18*).

High-purity trichloroethylene (TCE) and aniline (99.9%) were employed as the organic solutes, and lithium chloride was used as a tracer. The properties of the organic solutes are listed in Table 1. Stock solutions were prepared by dissolving both solutes into deionized water. Aqueous concentrations of TCE and aniline were assayed by using solvent extraction. Ether was selected as the solvent because it was capable of simultaneously extracting both compounds. The concentrations of organic solutes were analyzed by gas

* Corresponding author phone: (716) 645-2114 x 2327; fax: (716) 645-3667; e-mail: rabideau@eng.buffalo.edu.
† Present address: Chopra Lee, Inc., Grand Island, NY.

S0013-936X(97)00202-2 CCC: $15.00
Published on Web 03/26/1998

TABLE 1. Properties of Organic Solutes

solute	aqueous solubility[a] (mg/L)	aqueous diffusion coeff[a] (D_0) (cm^2/s)	molecular radius[b] (Å)	log K_{ow}[a]
TCE	1100	1.07×10^{-5}	3.49	2.29
aniline	35000	9.80×10^{-6}	3.65	0.90

[a] From Montgomery (*18*). [b] From Lebas volume (*19*) assuming spherical molecule.

chromatography using an Ni electron capture detector (TCE) or flame ionization detector (aniline) with nitrogen as the carrier gas. Aqueous chloride concentrations were measured using a Shimadzu ion chromatograph equipped with an anion exchange column. All of the analytical solvents were of reagent grade or better.

Column Transport Experiment. Flexible wall permeameters are routinely used to measure the hydraulic conductivity of barrier materials and to assess chemical compatibility with contaminated leachates (*2*). In a typical flexible wall permeameter, a cylindrical porous medium sample is confined by rigid caps on the ends and a flexible membrane on the sides. The enclosed sample is contained within a larger cylindrical glass cell that is filled with water and pressurized to exert a confining stress, which minimizes the potential for sidewall leakage. Flexible tubing is connected to the top and bottom end caps for the passage of the permeating fluid. The pressures of the influent, effluent, and confining fluids are monitored and controlled from a central panel. Contaminated liquids are isolated from the control panel using "bladder accumulators", which consist of glass chambers with flexible membranes that separate the permeant from the uncontaminated fluid used to control pressure. A schematic of the apparatus is shown in the supplemental figure (see Supporting Information). More detailed descriptions of the equipment are available elsewhere (*21, 22*).

In this study, four column experiments were performed under saturated conditions using commercial permeameters (Brainard-Kilman S-480). Prior to use, the permeameter cells were cleaned with a hot detergent water soak, a hot tap water rinse, and a deionized−distilled water rinse. In preparing each column, approximately 1000 g of the SB mixture was wet uniformly with deionized water and placed in a mold that formed the sample into a cylinder approximately 7 cm in diameter and 10−12 cm in length. Initially, the water content was approximately 10% higher than eventually achieved under saturated and consolidated conditions. The sides of the SB specimens were wrapped with three liners: an innermost Viton-coated nitrile membrane, a middle layer of aluminum foil, and an outer nitrile membrane. The multiple liner system was designed to reduce the potential for diffusion of contaminants into the confining water.

Porous stone diffusers are normally placed at the ends of the sample to promote uniform lateral distribution of the permeant. The significant quantity of fluid retained by these stones and the potential for contaminant sorption have been recognized by researchers as obstacles to rigorous modeling of contaminant breakthrough curves generated using flexible walls permeameter (*10*). Shackelford and Redmond (*11*) circumvented this difficulty by replacing the stone diffusers with several layers of filter paper but did not perform measurements to confirm that lateral mixing across the column cross-section was achieved. In this work, sections of nonsorbing glass wool were placed at the two ends of the columns, and appropriate measures were taken to verify lateral mixing and account for boundary effects in modeling (discussed below).

After placement of the specimen in the permeameter cell under an effective confining pressure of 28 kPa, saturation was achieved by gradually increasing the backpressure (applied at the ends of the column) to 315 kPa, in increments of 35 kPa. The specimen was allowed to saturate in accordance with ASTM 5084 until a Skempton's B parameter of over 0.95 was achieved. The hydraulic gradient was then applied by increasing the influent pressure, and the system was allowed to gradually come to equilibrium with respect to the confining pressure (sides of column). The process of backpressure saturation and stabilization of the hydraulic gradient required 3−4 weeks for each column run.

The aqueous solution of contaminants was introduced to the column after the ratio of the observed inflow and outflow rates remained within 10% for a period of 1 week, and negligible flow was observed in the buret connected to the confining fluid. Each transport experiment was initiated by filling the influent bladder accumulator with the feed solution and connecting it to the column influent port. Regular sampling of the influent was performed to record temporal variation in the influent boundary condition, and inflow and outflow rates were monitored to identify any change in hydraulic conductivity during the course of the experiments.

Column effluent samples were regularly monitored over the duration of each experiment, which varied from 25 to 49 days. After the desired elapsed time, four subsamples from the column were removed by inserting stainless steel tubes into the SB sample, which was placed in a rigid mold that prevented lateral movement of the SB during the coring process. The four cores consisted of a central core (1.8 cm in diameter) and three equidistant−equispaced radial cores (each 1.1 cm in diameter). The SB cores were extruded from the stainless steel tubes in segments of approximately 0.5 cm in length. After cutting with stainless steel wire, each segment was placed directly into a preweighed extraction vial containing a known volume of solvent. The vials were again weighed, and the length of each segment was confirmed from the mass of soil. The vials were vigorously shaken for 24 h, and the extract was analyzed to determine the total amounts of TCE and aniline present in the combined aqueous and sorbed phases, expressed as a total mass concentration M (mass of extracted solute per mass of solid material). The entire operation of extrusion and sectioning was accomplished in less than 5 min for each rod and yielded approximately 20 samples per core. Portions of the remaining SB sample were weighed and oven dried for 48 h at 105 ± 5 °C for the determination of porosity, bulk density, and solid density. The confining water, flexible membranes, and influent/effluent glass wool were also subjected to extraction and analysis for mass balance purposes.

Sorption Isotherms. Two sets of batch sorption experiments were conducted, for equilibration periods of 7 and 10 days. Aqueous solutions of the desired solutes were added to 12 mL glass vials containing 7 g of SB, leaving no headspace, and tumbled at approximately 28 rpm for the desired period. The samples were prepared in quadruplet (two with SB and two control) for mixtures at 10 concentration levels ranging from 0 to 200 and from 0 to 400 mg/L for TCE and aniline, respectively. Following the equilibration period, the vials were centrifuged at 5000 rpm for 90 min, and the liquid phase was extracted and analyzed. The sorbed mass was calculated as the difference between the initial and remaining mass in the aqueous phase, with the initial mass estimated from the controls. To assess mass balance, extraction of both the liquid and solid phases was performed for 21 additional sampling points.

Mathematical Model

A conceptual model for a vertical barrier system is that of a homogeneous one-dimensional (1D) porous media system

with a hydraulic gradient normal to the plane of the barrier. If linear equilibrium sorption is assumed, the general form of the ADR equation is

$$\left(1 + \frac{\rho_b K_d}{n}\right)\frac{\partial C}{\partial t} = -v\frac{\partial C}{\partial x} + D\frac{\partial^2 C}{\partial x^2} - \lambda C \qquad (2)$$

where C is the dissolved phase contaminant concentration, t is time, x is distance from the contaminated side of the barrier of thickness L, v is the average linear velocity, D is the dispersion coefficient (includes hydrodynamic dispersion and molecular diffusion), K_d is the sorption coefficient, ρ_b is the bulk density, and λ is the first-order decay constant for the aqueous phase.

The dispersion coefficient consists of two components:

$$D = a_l v + \frac{D_e}{n} \qquad (3)$$

where a_l is the medium dispersivity.

Performance of a barrier is frequently considered in terms of the contaminant flux (f):

$$f = nvC - nD\frac{\partial C}{\partial x} \qquad (4)$$

The measured spatial mass concentrations were related to the modeled aqueous concentrations using the assumed isotherm [$M = C\,(n + \rho_b K_d)$] (*12*).

Boundary Conditions. Adaptation of eq 2 to the analysis of column experiments requires careful consideration of the boundary conditions. In the experiments described here, glass wool was placed at the column entrance and exit boundaries to promote lateral mixing. Because of the small volume and high porosity of the glass wool, it was assumed that the pore fluid approached complete mixing within these transition zones. Furthermore, it was assumed that concentration gradients were negligible in the 0.32 cm diameter Teflon tubing connected to the column. Mass balance boundary conditions based on a uniform concentration inside the glass wool can therefore be defined as (*24*)

$$C(0, t) = \frac{Q}{V_{gi}}\int_0^t C_{in}(\tau)\,d\tau - \frac{A}{V_{gi}}\int_0^t f_0(0, \tau)\,d\tau \qquad (5)$$

$$C(L, \tau) = \frac{A}{V_{ge}}\int_0^t f(L, \tau)\,d\tau - \frac{Q}{V_{ge}}\int_0^t C(L, \tau)\,d\tau \qquad (6)$$

where V_{gi} and V_{ge} are the volumes of glass wool at the column inlet and outlet, respectively; Q is the flow rate; A is the cross-sectional area of the column; C_{in} is the time-varying influent concentration measured at the column entrance; $f_o(0,\tau)$ is the flux at the influent glass wool/SB interface; and $f(L,\tau)$ is the flux at the effluent SB/glass wool interface, with fluxes as defined by eq 4. The influent concentration declines over time because of the diffusion/sorption of contaminant into the upper chamber of the bladder accumulator (confirmed by the analysis of the chamber fluid and extraction of the separating membrane), and the measured concentrations were fitted with second-order polynomials with respect to time, defined as

$$C_{in}(t) = C_0 + C_1 t + C_2 t^2 \qquad (7)$$

where C_0, C_1, and C_2 are fitted constants.

The solution of eq 2 with the boundary conditions represented by eqs 5−7 was obtained by application of the Laplace transform and numerical inversion using the algorithm of Talbot (*25*). Details of the solution technique are available elsewhere (*24*).

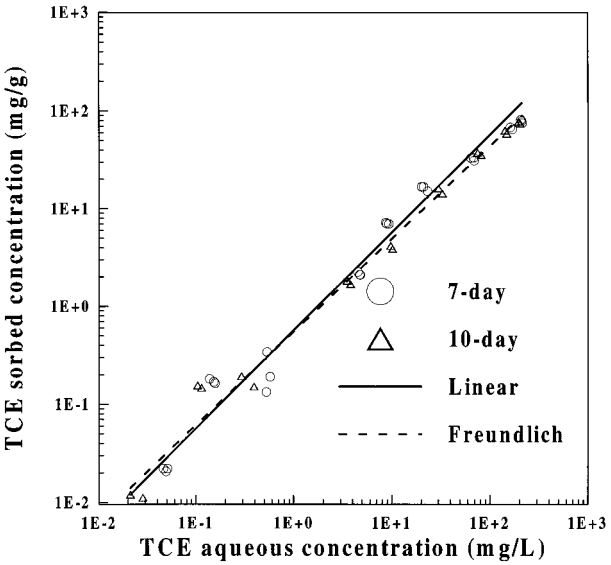

FIGURE 1. TCE sorption isotherms.

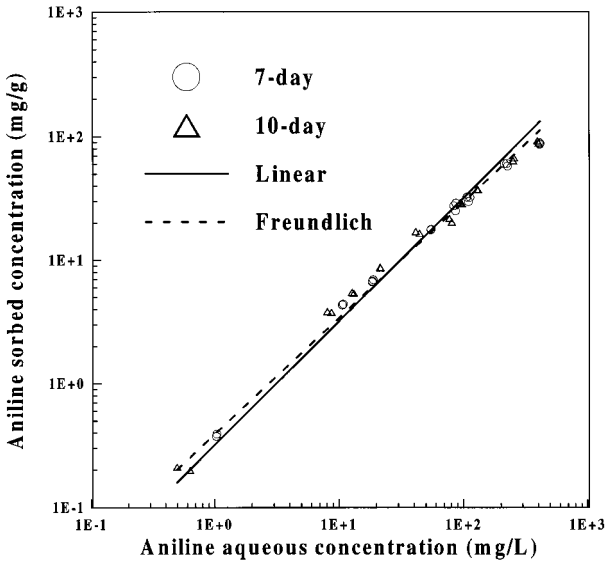

FIGURE 2. Aniline sorption isotherms.

Results

Sorption Experiments. Sorption of chloride was not observed in the batch experiments. Although the potential for competitive sorption was not considered explicitly in this work, the sorption of TCE and aniline was assessed using a mixture of both contaminants to replicate conditions present in the column transport experiments. The results for the 7- and 10-day isotherms were similar and were therefore combined into two data sets of 43 (aniline) and 45 (TCE) points, as shown in Figures 1 and 2 along with the linear and Freundlich fits. The mass recovery for the 21 samples subjected to total extraction was 98.2 ± 4.2%, suggesting that volatilization losses were minor. The isotherm constants (Table 2) were estimated by regression according to the procedures discussed by Ball and Roberts (*26*), based on the assumption of constant relative error in the estimated sorbed concentrations. As expected, the more hydrophobic TCE exhibited greater sorption. While the Freundlich isotherm yielded better fits, the degree of nonlinearity was minor (exponents ~0.91−0.96). Test simulations performed using

TABLE 2. Batch Isotherm Parameters

compound	duration	no. of points	linear ($q = K_d C$)[a] K_d (cm³/g) (95% CI)	Freundlich ($q = K_F C^n$) K_f (cm³/g)^{nf} (95% CI)	n_f
TCE	7-day	27	0.59 (0.48, 0.68)	0.55 (0.43, 0.71)	0.96 (0.89, 1.03)
	10-day	18	0.56 (0.43, 0.69)	0.53 (0.41, 0.70)	0.94 (0.86, 1.02)
	combined	45	0.57 (0.49, 0.65)	0.53 (0.44, 0.66)	0.95 (0.90, 1.00)
aniline	7-day	23	0.32 (0.28, 0.36)	0.41 (0.30, 0.58)	0.91 (0.86, 1.00)
	10-day	20	0.33 (0.29, 0.37)	0.38 (0.28, 0.53)	0.92 (0.85, 0.99)
	combined	43	0.33 (0.29, 0.37)	0.36 (0.28, 0.49)	0.93 (0.88, 1.00)

[a] q = sorbed phase mass fraction (mg/g); C = aqueous concentration (mg/L).

TABLE 3. Summary of Column Experimental Conditions

parameter	comment	experiment 1a	1b	2	3	4
contaminant		chloride	TCE/aniline	TCE/aniline	TCE/aniline	TCE/aniline
duration (days)		45	45	25	49	25
hydraulic conductivity (K_h) $\times 10^8$ (cm/s)	measured in permeameter	1.01	1.01	2.27	1.28	2.19
column length (cm)		11.3	11.3	12.4	10.9	12.9
hydraulic gradient	Average	66.5	66.5	5.3	3.1	5.1
porosity (n)	Average	0.321	0.321	0.337	0.341	0.339
glass wool vol (V_g) (mL)	Average	9.97	9.92	9.88	10.21	10.13
C_oTCE (mg/L)	fitted from influent measurements	4064[a]	496.1	451.9	442.9	445.2
C_1TCE (mg/L-d)		0[a]	−4.11	−11.4	0.335	0.330
C_2TCE (mg/L-d^2)		0[a]	0.0087	0.258	−0.047	−0.053
$C_o^{aniline}$ (mg/L)	fitted from influent measurements		723.9	1038.75	1059.5	1057.2
$C_1^{aniline}$ (mg/L-d)			−6.59	−3.34	−1.76	−1.92
$C_2^{aniline}$ (mg/L-d^2)			0.047	0.031	−0.001	−0.003

[a] For chloride in experiment 1.

a numerical model (*24*) yielded similar predicted contaminant profiles for the two isotherm models. In light of the observed differences between batch and column conditions (discussed below), the linear isotherm was adopted to reduce the number of required calibration parameters.

Column Transport Experiments. Four SB column experiments were conducted according to the conditions summarized in Table 3. Experiment 1 was conducted in stages using two solutes introduced sequentially: lithium chloride (experiment 1a) and TCE/aniline (experiment 1b). A very high hydraulic gradient was used in experiment 1 (66.5) to produce effluent breakthrough within a reasonable time frame, while experiments 2−4 were performed at lower hydraulic gradients that were closer to typical field conditions. Effluent concentrations of all solutes and spatial contaminant mass profiles of the organic solutes were measured in all experiments, although TCE/aniline were not detected in the effluent for experiments 2−4.

Column flow rates and hydraulic gradients were measured periodically and remained within ±10% of the original value for all experiments. As shown in Table 3, the observed average hydraulic conductivities were on the order of 10^{-8} cm/s, which is lower than commonly cited design standards of 10^{-7} cm/s but within the range reported for installed slurry walls (*2*). The average porosity measured in experiment 1 was lower than the remaining experiments, presumably due to the increase in confining pressure associated with the higher applied hydraulic gradient. Declines in the influent concentrations of organic solutes were noted and described by second-order polynomials, as summarized in Table 3.

For each column, the four cores were sectioned and extracted, including a central core and three smaller diameter outer cores. The extracted mass for equidistant segments was within ±5% for all samples, and the 1D modeling approach was therefore deemed suitable. The estimated total mass recovery for the various experiments varied between 84 and 88% for TCE and between 93 and 96% for aniline.

Modeling of Column Experiments. Modeling was performed using the effluent concentrations (experiment 1) and the spatial mass data from the central cores (all experiments). The unaccounted for mass was attributed to volatilization losses during the extrusion and sectioning of the column and/or incomplete extraction of the segments. Therefore, the spatial data were transformed by dividing by the fraction of chemical recovered for each experiment. Although there was no evidence to suggest the occurrence of significant transformation reactions within the columns, modeling was also performed by using the untransformed data and fitting a first-order decay term in the transport model. Both approaches yielded similar calibrations of sorption and dispersion coefficients (±10%); since the loss of contaminants during the sectioning and extraction process was considered a more likely scenario, only those results are reported here.

The maximum neighborhood algorithm of Marquardt (*27*) was used for nonlinear regression of eq 1, with multiple initial guesses. Due to the potential volatilization of organic solutes during the extrusion and sectioning of the cores, the errors for the spatial mass concentrations were expected to be roughly proportional to the measured values, and the squared *relative* deviations were therefore minimized (*28*). However,

TABLE 4. Column Parameter Estimates

		four-parameter fit				two-parameter fit			
colum (no. of pts)	compound	$D_e/n \times 10^6$ (cm^2/s)	Hp	K_d (cm^3/g)	SS[b]	$D_e/n \times 10^6$ (cm^2/s)	Hp	K_d (cm^3/g)	SS
1 (10)	chloride[a] (effluent)	5.51	2.47		19617				
(10)	TCE (effluent)	4.19	2.55	0.11	26.4	3.71	2.88	0.13	145.8
(23)	TCE (spatial)	3.97	2.70	0.05	0.7	4.38	2.44	0.13	1.7
(10)	aniline (effluent)	3.85	2.54	0.10	5.1	3.70	2.88	0.08	117.8
(23)	aniline (spatial)	3.64	2.69	0.12	0.3	4.01	2.44	0.08	0.9
2 (17)	TCE	3.77	2.84	0.005	0.6	3.12	3.42	0.05	4.8
(17)	aniline	2.06	4.75	0.0	1.5	2.86	3.42	0.03	3.4
3 (20)	TCE	2.48	4.31	0.0	1.8	1.89	5.66	0.11	4.5
(20)	aniline	1.07	9.15	0.0	1.1	1.73	5.66	0.06	2.5
4 (18)	TCE	4.72	2.27	0.091	1.3	2.43	4.41	0.01	4.6
(18)	aniline	1.67	5.86	0.0	1.7	2.22	4.41	0.006	2.1

[a] Chloride results based on single parameter fit, with aqueous diffusion coefficient for LiCl = 1.36×10^{-5} (4). [b] SS, sum of squared deviations = Σ(model − data)^2 computed using effluent concentrations (C) or natural log of total mass (ln M) for spatial profiles.

for the aqueous effluent concentrations, the measurement errors were assumed normal with uniform variance, and *absolute* deviations (standard least squares) were therefore used (*29*).

Estimates of the sorption coefficients (K_d) and dispersion coefficients (D) for both TCE and aniline were necessary to simulate the results of the SB column transport experiments. Initial attempts were made to model the column data using sorption parameters obtained from the batch experiments. This approach was rejected, however, because the calibrated dispersion coefficients (D) were consistently of the same order or higher than the contaminant free liquid diffusion coefficient (i.e., 80−150% D_o). Based on preliminary modeling results, two approaches were selected for model calibration. In the first approach, the model parameters D and K_d were independently calibrated for TCE and aniline for each experiment (a four-parameter fit). In the second approach, the sorption coefficients were simultaneously calibrated for TCE and aniline by fixing the ratio of sorption coefficients for TCE and aniline to that measured in the batch experiments, neglecting the hydrodynamic component of dispersion ($a_L v$ in eq 3) and fitting a single hindrance for both contaminants (a two-parameter fit). The assumption of equal hindrance was adopted because of the similarity in molecular radius for TCE and aniline, which implies similar effects from steric and viscous forces (*30, 31*).

The parameter estimates for all experiments are summarized in Table 4. The calibrated dispersion coefficients (D) were interpreted in terms of diffusion (D_e/n) by neglecting the hydrodynamic term. The data and model fits for the chloride and TCE effluent profiles from experiment 1 are shown in Figure 3; the aniline data were very similar to the TCE data and are not shown. The spatial mass profiles for the organic solutes exhibited similar trends for all experiments; therefore, for illustrative purposes, only the results from experiment 2 are shown in Figures 4 and 5. In general, calibration of both the dispersion coefficient and sorption coefficient for each solute (four-parameter fit) resulted in close agreement between the predictions and the data, with deviations associated with scatter in the data rather than systematic trends. When the calibration was constrained (two-parameter fit), the quality of the fits declined and systematic deviations were apparent, particularly for TCE in the low-gradient experiments (Figure 4).

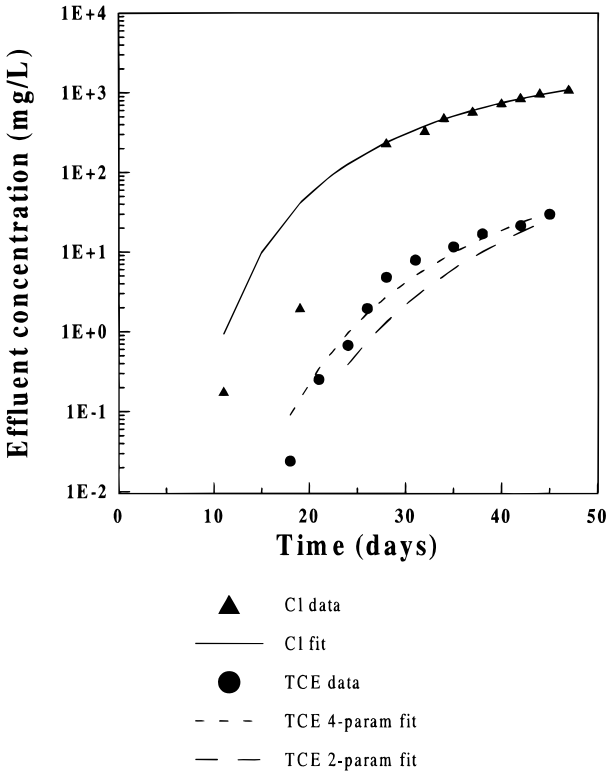

FIGURE 3. Observed and fitted effluent breakthrough curves from experiment 1.

Discussion

In general, the effective diffusion coefficients measured in this study are within the range observed by others for earthen barrier materials (*9−11, 17*), although variability across experiments and calibration approaches was noted. However, regardless of the calibration approach, the corresponding hindrance factors are larger than predicted using Millington's correlation ($Hp = 1.46$ for $n = 0.34$), which was endorsed by Mott and Weber (*12, 33*; hereafter denoted as M&W) for SB materials. Differences in materials, experimental methods, and data interpretation strategies preclude an in-depth comparison of this study with the work of M&W. However, theoretical calculations performed by M&W suggested that steric hindrance should contribute to the overall hindrance for the solutes and SB materials used in both studies. Because Millington's analysis addressed only the extended diffusion path caused by a tortuous porous medium geometry and ignored steric and other hindrance factors, it is not surprising that lower effective diffusion coefficients were observed. From the range of results observed in this study and M&W's work, it may be tentatively concluded that Millington's correlation would produce conservative (high) preliminary estimates for effective diffusion coefficients for organic contaminants in SB.

The scatter in diffusion and sorption coefficients noted in Table 4 is somewhat correlated with the experimental flow

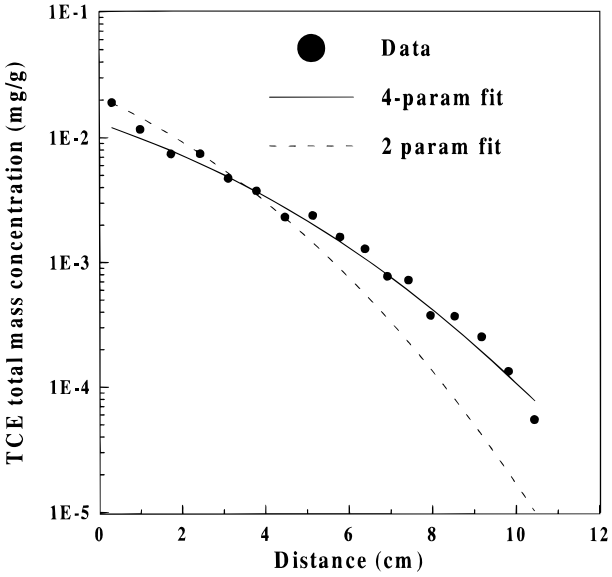

FIGURE 4. Observed and fitted TCE spatial mass profiles from experiment 2.

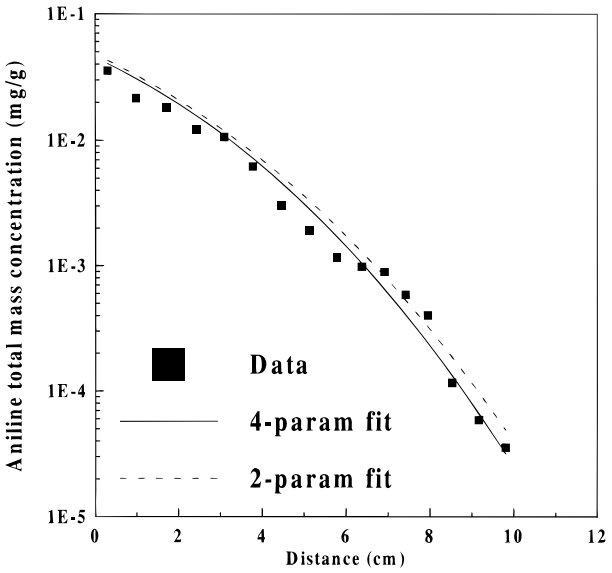

FIGURE 5. Observed and fitted aniline spatial mass profiles from experiment 2.

rates and durations. Although low column flow rates are appealing because of the closer correspondence with expected field conditions, the diffusion and sorption parameters are more strongly correlated in the automated parameter estimation process. This correlation is reduced as the degree of advection is increased in the governing transport equation. In this work, the experiment with the highest flow rate (experiment 1) yielded estimated hindrance factors that were reasonably consistent across the three solutes as well as between the spatial and temporal profiles. The lesser degree of parameter correlation is also indicated by the similarities between the two- and four-parameter fits for this experiment. The hindrance factors for experiment 1 are smaller than those estimated for the other experiments. This difference could be influenced by the correlation in the parameter estimation process for the lower gradient experiments or could be due to actual differences between the columns. For example, the higher flow rates used in experiment 1 could have resulted in a hydrodynamic mixing contribution to dispersion, although the data are not sufficient to test this hypothesis.

One of the primary observations of this work is the difference between the sorption constants estimated from the batch and column experiments. Although there was significant scatter in the column estimates, the highest estimated K_d values (experiment 1) were significantly less than the corresponding batch measurements. The relative agreement in the various calibrated sorption coefficients for this experiment (temporal versus spatial, two-parameter versus four-parameter) suggests that the small calibrated sorption coefficients are not artifacts of the parameter estimation process. One possible contributing factor is the well-known dependence of K_d on the soil-to-solution ratio in batch isotherm experiments (*32, 34, 35*). In the SB experiments presented here, the solid-to-liquid ratios applicable to the column experiments are approximately twice those of the batch experiments. Another explanation is the potential for nonequilibrium sorption in the columns, which could influence the formation of bentonite gel under consolidated conditions (*12, 23, 36*). The gel would represent an additional resistance to the transport of solute molecules to the sorbing matrix, and resulting kinetic effects and reduced effective porosity would be inconsistent with the model expressed by eq 2. The possibility of nonequilibrium is supported by the observation that the largest calibrated K_d values were associated with the experiments of the longest duration (experiment 1 and two-parameter calibrations for experiment 3).

Only two published studies were located in which both batch and column experiments were performed with SB, and for comparison purposes, data from these studies were obtained and analyzed using the modeling approach described above. In experiments performed by Bierck and Chang (*37*), the observed column breakthrough curves for 2-propanone in SB modified with activated carbon could not be accurately predicted using eq 2 unless the sorption coefficient was reduced by approximately a factor of 2 from the independently measured batch value. Similar reductions in the sorption coefficient were required to accurately predict the transport of lindane through SB amended by fly ash in the study of M&W (*34*). For either of these studies, adoption of the average measured batch sorption coefficient would result in a significant underprediction of the degree of contaminant penetration into the SB barrier using a local equilibrium model. As discussed by Rabideau and Khandelwal (*24*), inclusion of a kinetic sorption significantly improved modeling predictions of the M&W experiments with fly ash-amended SB. For the present study, similar numerical experiments were performed using a two-region kinetic model. While some improved model calibrations were obtained, it was felt that the experimental design used in this work (single-time spatial profiles) precluded unique multiparameter estimation, and these results are not presented.

With the renewed interest in containment technology, it is likely that contaminant transport modeling will play a more central role in the design of vertical barriers, and estimates of diffusion and sorption parameters will be required. Because the correlation proposed by Millington yields hindrance factors at the low end of the range of values observed and calculated in this study and by other researchers, it may serve as a useful conservative starting point for the design of barrier systems. Furthermore, the amount of sorption of organic contaminants in unamended SB is likely to be small, so it may also be expedient and conservative to simply neglect sorption in the analysis of these systems. For barrier materials amended with sorbing additives, however, more research is needed to develop and test appropriate conceptual and mathematical models. If actual medium-specific measurements are required, the use of standard flexible wall permeameters may be a cost-effective approach for obtaining these data, provided that suitable precautions

are taken to ensure lateral mixing and appropriately model the resulting boundary conditions. However, further work is necessary to clarify the role of nonequilibrium sorption and to develop experimental designs that support robust parameter estimation.

Acknowledgments

Funding for this research was provided by DuPont. In particular, we thank Dr. Calvin Chien, Containment and Transport Modeling Team Leader, for his support and input to this project. Portions of this work were presented at the International Containment Technology Conference and Exhibition, St. Petersburg, FL, February 8-10, 1997. We also thank Henry Mott and Barnes Bierck for providing experimental data from earlier studies.

Supporting Information Available

A figure showing the schematic of the SB column apparatus (1 p) will appear following these pages in the microfilm edition of this volume of the journal. Photocopies of the Supporting Information from this paper or microfiche (105 × 148 mm, 24× reduction, negatives) may be obtained from Microforms Office, American Chemical Society, 1155 16th St. NW, Washington, DC 20036. Full bibliographic citation (journal, title of article, names of authors, inclusive pagination, volume number, and issue number) and prepayment, check or money order for $12.00 for photocopy ($14.00 foreign) or $12.00 for microfiche ($13.00 foreign), are required. Canadian residents should add 7% GST. Supporting Information is also available via the World Wide Web at URL http://www.chemcenter.org. Users should select Electronic Publications and then Environmental Science and Technology under Electronic Editions. Detailed instructions for using this service, along with a description of the file formats, are available at this site. To download the Supporting Information, enter the journal subscription number from your mailing label. For additional information on electronic access, send electronic mail to si-help@acs.org or phone (202)872-6333.

Literature Cited

(1) Rumer, R. R., Ryan, M., Eds. *Review and Evaluation of Containment Technologies for Remediation Applications*; John Wiley & Sons: New York, 1994.
(2) Rumer, R. R., Mitchell, J., Eds. *Assessment of Barrier Containment Technologies* NTIS PB96-180583; 1996.
(3) Rowe, R. K. In *Geotechnical Practice for Waste Disposal*; Woods, R., Ed.; ASCE: New York, 1987; pp 159−189.
(4) Shackelford, C. D. *Transport. Res. Rec.* **1989**, *1219*, 169−182.
(5) Gray, D. G.; Weber, W. J., Jr. *Proceedings of the Seventh Annual Madison Waste Conference;* University of Wisconsin-Extension: Madison, WI, 1984.
(6) Goodal, D. C.; Quigley, R. M. *Can. Geotech. J.* **1977**, *14*, 223−236.
(7) Crooks, V. E.; Quigley, R. M. *Can. Geotech. J.* **1984**, *21*, 349−362.
(8) Desaulniers, D. E.; Cherry, J. A.; Fritz, P. *J. Hydrol.* **1981**, *50*, 231−257.
(9) Johnson, R. L.; Cherry, J. A.; Pankow, J. F. *Environ. Sci. Technol.* **1989**, *23*, 340−349.
(10) Acar, Y. B.; Haider, L. *J. Geotech. Eng.* **1990**, *116*, 1031−1052.
(11) Shackelford, C. D.; Redmond, P. L. *J. Geotech. Eng.* **1995**, *121* (1), 17−32.
(12) Mott, H.; Weber, W. *Environ. Sci. Technol.* **1991**, *25*, 1708−1715.
(13) Millington, R. J. *Science* **1959**, *130*, 100−102.
(14) Wakao, N.; Smith, J. M. *Chem. Eng. Sci.* **1962**, *17*, 825.
(15) Gratwohl, P.; Reinhard, M. *Environ. Sci. Technol.* **1993**, *27*, 2360−2366.
(16) Gillham, R. W.; Robin, M. J. L.; Dytynyshyn, D. J.; Johnston, H. M. *Can. J. Geotechnol.* **1984**, *21*, 541−550.
(17) D'Appolonia, D. J. *ASCE J. Geotech. Eng. Div.* **1980**, *106*, 399−417.
(18) Schulze, D.; Barvenik, M.; Ayers, J. *Proceedings of the Fourth National Symposium and Exposition on Aquifer Restoration and Groundwater Monitoring,* Columbus, OH, 1984.
(19) Montgomery, J. H. *Groundwater Chemicals*; Lewis Publishers: Boca Raton, FL, 1996.
(20) Tucker, W. A.; Nelken, L. A. In *Handbook of Chemical Property Estimation Methods*; Lymann, W. J., Reehl, W. F., Rosenblatt, D. H., Eds.; McGraw-Hill: New York, 1982.
(21) Daniel, D. E. *ASCE J. Geotech. Eng. Div.* **1984**, *110* (2), 285−300.
(22) Evans, J. C.; Fang, J. Y. *ASTM Spec. Technol. Publ. 977* **1988**, 387−404.
(23) Smith, J. A.; Jaffe, P. R. *J. Environ. Eng.* **1994**, *120* (6) 1559−1577.
(24) Rabideau, A. J.; Khandelwal, A. *J. Environ. Eng.* In press.
(25) Talbot, A. *J. Inst. Math. Appl.* **1979**, *23*, 97−120.
(26) Ball; Roberts. *Environ. Sci. Technol.* **1992**, *26* (6), 1234−1242.
(27) Marquardt, D. W. *J. Appl. Math.* **1963**, *11*, 431−441.
(28) Deak, A.; Kemeny, S. *Fluid Phase Equilibria* **1994**, *100*, 171−190.
(29) Bevington, P. R. *Data Reduction and Error Analysis for the Physical Sciences;* McGraw-Hill: New York, New York, 1969.
(30) Satterfield, C. N.; Colton, C. K.; Pitcher, W. H., Jr. *AIChE. J.* **1973**, *19* (3), 628−635.
(31) Smith, D. M. *AIChE J.* **1986**, *32* (6), 1039−1042.
(32) Barone, F. S.; Rowe, R. K.; Quigley, R. M. *J. Contam. Hydrol.* **1992**, *10*, 225−250.
(33) Mott, H.; Weber, W. *Environ. Sci. Technol.* **1992**, *26* (6), 1234−1242.
(34) Grover, R.; Hance, R. J. *Soil Sci.* **1970**, *109*, 136−138.
(35) Gschwend, P. M.; Wu, S. *Environ. Sci. Technol.* **1985**, *19*, 70−96.
(36) Mollins, L. H.; Stewart, D. I.; Cousens, T. W. *Clay Miner.* **1996**, *31*, 243−252.
(37) Bierck, B. R.; Chang, W. C. *Proceedings of the Water Environment Specialty Conference on Innovative Solutions for Contaminated Site Management*, Miami, 1994; pp 461−472.

Received for review March 7, 1997. Revised manuscript received September 30, 1997. Accepted February 4, 1998.

ES9702024